AEEJ : Journal of Automotive Engineering and Vocational Education
Volume: 06, Number: 01, 2025
ISSN: 2722-4031 [online]; 2722-404X [printed]
DOI: https://doi.org/10.24036/aeej.v6i1.300

Analysis the Effect of Variation Permanent Magnet and Winding on BLDC Motor Performance Using ANSYS Maxwell Simulation

Muhamad Yusron Nur Arna[1]*, Dony Hidayat Al-Janan[1]

Abstract

One of the driving components of electric vehicles that are often used is Brushless (BLDC) motors which have advantages such as high efficiency, large torque density, and precise speed control. This study aims to evaluate the effect of variations in permanent magnet type and stator winding configuration on the performance of Brushless DC (BLDC) motors. Two types of permanent magnets, NdFe35 and SmCo24, are compared based on their electromagnetic characteristics, such as torque, rotational speed, efficiency, and current consumption. In additional, the stator winding parameters were varied, including wire diameters between 1.3 mm and 1.6 mm and the number of conductors per slot between 14 and 23. The simulation results conducted using ANSYS Maxwell show that the configuration combining NdFe35, an optimal number of 14 conductors per slot, and a large wire diameter of 1.6 mm delivers the best performance, with a maximum torque of 325 Nm, maximum power of 2.91 kW, efficiency of 79%, and a speed of 1241.5 rpm. Although the current consumption is high, the resulting power and torque performance are proportional.

Keywords
BLDC, ANSYS, Permanent Magnet, Number of turns, Maxwell, Torque

[1] Departement of Mechanical Engineering, Faculty of Engineering, Universitas Negeri Semarang
Sekaran, Kecamatan Gn. Pati, Kota Semarang, Jawa Tengah
** myusronna@students.unnes.ac.id*

Submitted : July 25, 2025. Accepted : Augustus 16, 2025. Published : December 31, 2025

INTRODUCTION

Electric vehicles (EVs) have been developed for decades in response to various global challenges, including climate change, depletion of fossil fuels, deteriorating air quality, and other environmental issues [1]. These concerns have driven industries to transition from internal combustion engine vehicles to electric alternatives. In many countries especially urban areas transportation remains a major contributor to harmful emissions, including pollutants such as particulate matter (PM), nitrogen dioxide (NO_2), carbon monoxide (CO), and sulfur dioxide (SO_2), all of which pose significant public health risks [2]. Transitioning to clean energy ecosystems is considered a promising approach to reduce fossil fuel consumption and greenhouse gas emissions.

One of the most commonly used components in EV propulsion systems is the brushless direct current (BLDC) motor. BLDC motors offer numerous advantages, such as high torque, absence of brush-related losses, low inertia, excellent speed control, and higher efficiency compared to stepper motors [3]. However, challenges such as complex circuitry and high manufacturing costs remain, indicating a need for further development. BLDC motors are sensor-controlled synchronous machines powered by direct current, widely adopted in the automotive, medical, and automation industries due to their high efficiency and performance [4][5]. Their compact design enables easy integration into complex systems such as electric vehicles. With continuous advancements in technology, BLDC motors are projected to play a key role in the development of sustainable industrial applications in the near future [6]. Research on BLDC motor optimization continues to be a critical area within electrical and automotive engineering [7]. Improving performance metrics particularly torque and rotational speed remains a key focus. Among the factors that influence BLDC motor performance, permanent magnet material and stator winding geometry stand out. Magnet type affects torque characteristics and magnetic field strength, while wire diameter impacts resistive losses, current-carrying capacity, and overall efficiency [8].

Permanent magnets are essential components in BLDC motors due to their ability to generate stable magnetic fields without requiring external power. Their energy efficiency makes them ideal for use in high-performance electric machines [8][9]. Several types of permanent magnets (PMs) have been studied in previous research, including AlNiCo, NdFe30, NdFe35, and SmCo24 [10][11]. These magnets vary in magnetic flux density, energy product, and thermal resistance. Moreover, the structural configuration of the magnets, such as surface-mounted perpendicular to the rotor shaft, parallel alignment, or bread-shaped magnets affects flux distribution and energy conversion efficiency [12][13]. Figure 1 illustrates these three magnet structures, each offering unique advantages in terms of torque density, compactness, and thermal characteristics.

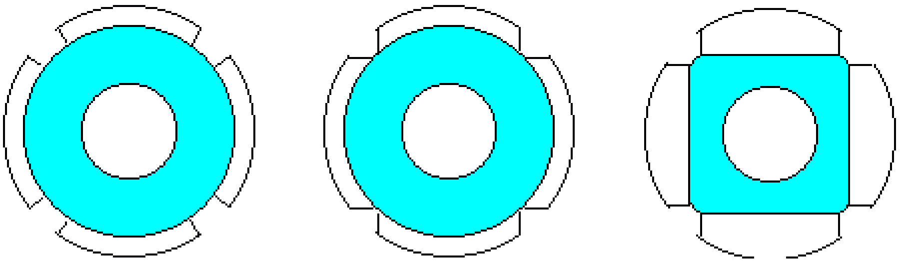

a) **b)** **c)**

Figure 1. Various magnetic surface rotor structures, a) surface magnets perpendicular to the rotor shaft, b) surface magnets parallel to the rotor shaft, c) bread-shaped magnets [5].

Similarly, the slot geometry within the stator is a critical design element, as it accommodates the windings and affects electromagnetic distribution [14]15]. Optimally sized slots reduce magnetic losses, improve torque smoothness, and minimize vibration and acoustic noise. Simulation tools like ANSYS Maxwell allow for accurate analysis of slot configurations prior to production. In this study, Slot Type 4 was selected for its balanced performance characteristics and suitability for electric vehicle applications (Figure 2).

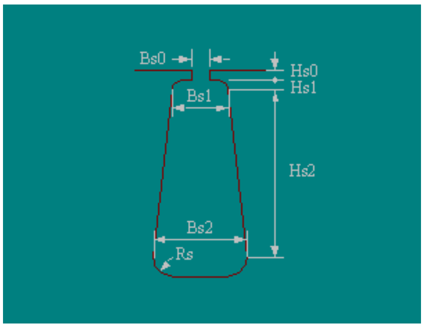

Figure 2. The type of slot used

Previous studies have investigated various factors affecting BLDC motor performance, such as rotor geometry, magnet type, and control techniques. For example, researchers have examined the impact of magnet shape on torque performance and cogging torque [10], and others have applied the Taguchi method to evaluate permanent magnet types (e.g., NdFe30, NdFe35, SmCo24) for torque ripple reduction and efficiency improvement [11]. Additionally, the optimization of stator slot dimensions and coil diameters has been shown to enhance operational stability and energy efficiency [16].

Despite extensive research on individual design parameters, limited studies have addressed the combined effect of magnet material, winding diameter, and conductor count per slot on overall motor performance, particularly with respect to torque, efficiency, and electromotive force (EMF). This study seeks to address that gap. Accordingly, this research investigates the effects of two permanent magnet types, NdFe35 and SmCo24, combined with variations in wire diameter and conductor count, on the electromagnetic performance of a BLDC motor. NdFe35, known for its high magnetic flux density and energy product, is applied in configurations A1 to A4, while SmCo24, valued for its thermal stability, is used in configurations B1 to B4 [12]. The wire diameters tested range from 1.3 mm to 1.6 mm, and conductor counts from 14 to 23. While higher conductor counts can improve EMF and magnetic flux, they also increase resistance, which may lead to thermal losses and reduced efficiency. Prior studies confirm the significant impact of these variables on electric motor efficiency [17][18].

To evaluate these effects, a numerical simulation using ANSYS Maxwell was employed as the primary method, offering precise electromagnetic analysis without the need for physical prototyping [19]. A total of eight motor configurations (A1–B4) were simulated and compared to assess the extent to which magnetic material and winding geometry influence BLDC motor performance. The findings aim to contribute to the design of more efficient and optimized BLDC motors for use in environmentally friendly, energy-efficient electric vehicle systems.

METHOD

This study employed a numerical electromagnetic simulation method to evaluate the performance of a brushless direct current (BLDC) motor using ANSYS Maxwell software. The primary objective was to analyze the effect of varying coil winding parameters on torque and rotational speed, based on predefined design specifications, as shown in Table 1. The simulation model was constructed using geometric data commonly found in light electric vehicle motors and previously validated in related studies [8][20]. Eight different motor configurations were simulated, each varying in three key parameters: type of permanent magnet, winding wire diameter, and number of conductors per slot. These variations were intended to assess their influence on key motor performance metrics, including torque, maximum power output, efficiency, and current consumption. Two types of permanent magnets were used: NdFe35 and SmCo24, each applied in four distinct configurations. Copper wire was selected as the winding material due to its high conductivity, with diameters of 1.3 mm, 1.45 mm, and 1.6 mm, and conductor counts ranging from 14, 15, 20, to 23 per slot.

Table 1. Configuration of conducted research

Configuration	***A1***	***A2***	***A3***	***A4***	***B1***	***B2***	***B3***	***B4***
Magnet type	NdFe35	NdFe35	NdFe35	NdFe35	SmCo24	SmCo24	SmCo24	SmCo24
Wire diameter (mm)	1.45	1.45	1.3	1.6	1.45	1.45	1.3	1.6
Conductor per slot	15	20	23	14	15	20	23	14

Motor Design Specifications

The BLDC motor used in this study was designed with a rated power of 1500 W and an operating voltage of 48 V. The motor featured 16 poles, which is typical for light electric vehicle applications in Indonesia. Detailed design specifications are summarized in Table 2.

Table 2. Machine geometri design

Parameter	***Value***
Rated output power (W)	1500
Rated voltage (V)	48
Number of pole	16
Windage loss (W)	20
Frictional loss (W)	10

Stator and Rotor Geometry

The stator and rotor were designed based on the specifications listed in Table 3 and 4. The stator featured 24 slots, an outer diameter of 210 mm, an inner diameter of 110 mm, and an axial length of 50 mm. The stator material was Steel_1010, with a stacking factor of 0.95. Copper wire was used for the windings to ensure optimal electrical conductivity. The rotor had an outer diameter of 108 mm, an inner diameter of 40 mm, and a length of 50 mm, with magnet thickness set at 4 mm. The rotor was also constructed from Steel_1010, offering the structural integrity required for high-speed operation. Figure 3 illustrates the motor geometry, including the stator, rotor, and overall layout. This structural configuration enables detailed analysis of how variations in winding parameters and magnet types influence overall motor performance [21].

Table 3. Stator geometri design

Parameter	***Value***
Number of slots	24
Outer diameter	210 mm
Inner diameter	110 mm
Length	50 mm
Stacking factor	0.95
Material	Steel_1010
Conduction type	Copper

Table 4. Rotor geometri design

Parameter	***Value***
Outer diameter	108 mm
Inner diameter	40 mm
Stacking factor	0.95
Length	50
Material	Steel_1010
Magnet thickness	4 mm

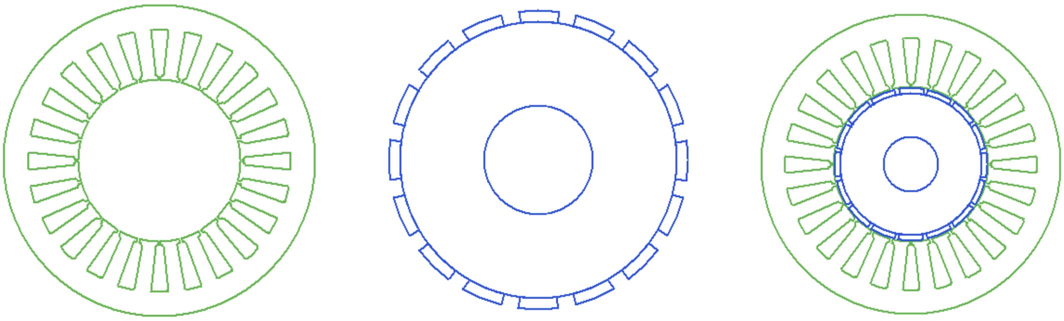

a) **b)** **c)**

Figure 3. Geometric drawings used a) stator design, b) rotor design, c) overall design.

Winding Configuration

The motor employed a whole-coiled distributed winding configuration, in which each phase was evenly distributed across the stator slots. The windings were arranged in a three-phase, symmetrical configuration, designed to produce a balanced rotating magnetic field. Single-strand copper wire was used, with diameters of 1.3 mm, 1.45 mm, and 1.6 mm across different configurations. To evaluate the impact of winding count on motor performance, multiple turns were tested, specifically 14, 15, 20, and 23 turns per slot. For configurations with 14 and 23 turns, adjustments were made based on wire diameter to ensure proper fit within the stator slots without exceeding maximum fill capacity. These variations were carefully managed to maintain slot compatibility and preserve the structural and electromagnetic balance of the system.

RESULT AND DISCUSSION

Maximum and Average Torque Comparison

The comparison of maximum and average torque for the eight BLDC motor configurations, based on RMxprt simulation results, is presented in Figure 4.

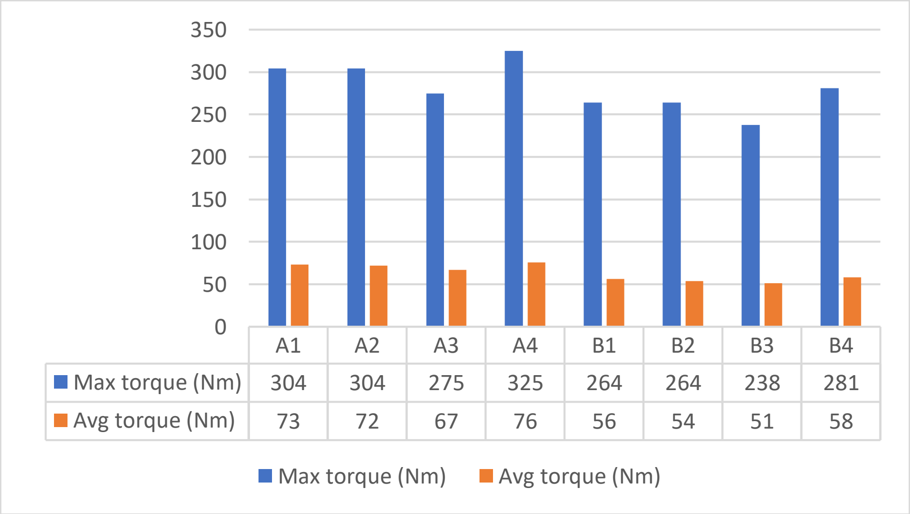

	A1	A2	A3	A4	B1	B2	B3	B4
🟦 Max torque (Nm)	304	304	275	325	264	264	238	281
🟧 Avg torque (Nm)	73	72	67	76	56	54	51	58

Figure 4. Maximum and average torque diagrams

Figure 4 shows the maximum and average torque values obtained from each simulated configuration. Among all configurations, A4 (NdFe35 magnet, 14 conductors, 1.6 mm wire diameter) achieved the highest performance, with a maximum torque of 325 Nm and an average torque of 76 Nm. Configurations A1 and A2 followed with maximum torque values of 304 Nm, and average torque values of 73 Nm and 72 Nm, respectively. These results indicate that the NdFe35 magnet consistently delivers superior torque performance compared to SmCo24-based configurations.

In contrast, configurations B1–B4, which use SmCo24 magnets, demonstrated lower torque output, with maximum torque ranging from 238 Nm to 281 Nm, and average torque ranging from 51 Nm to 58 Nm. Among them, B3 recorded the lowest performance, with a maximum torque of 238 Nm and an average of 51 Nm. The reduced torque in the SmCo24 configurations is primarily due to the lower magnetic flux density of SmCo24 compared to NdFe35. A weaker magnetic field results in reduced electromagnetic force within the motor, thereby lowering torque generation. Moreover, configurations with higher conductor counts, such as A3 and B3, both with 23 conductors exhibited a decline in average torque. This is attributed to increased winding resistance and reduced effective current. Although using thinner wire enables more conductors to fit in a slot, it also leads to higher resistance, decreasing current-carrying capacity and hence torque output. Conversely, configurations using thicker wires, such as in A4, resulted in lower resistance and improved current conduction, thus delivering higher torque output. These configurations struck a better balance between magnetic field strength and electrical efficiency.

Furthermore, Figure 5 presents the torque–speed curve of configuration A4 (NdFe35 magnet, 14 conductors, 1.6 mm wire diameter), which showed the best overall performance among all eight test cases. This configuration reached a peak torque of 325 Nm and sustained the highest average torque of 76 Nm. For comparison, configurations A1 and A2, which also used NdFe35 magnets but with more conductors (20 and 15) and smaller wire diameters (1.45 mm), achieved lower peak torque values of 304 Nm and average torque ranging from 72 Nm to 73 Nm. All configurations with SmCo24 magnets (B1 to B4) exhibited lower torque performance, with maximum torque peaking at 281 Nm and average torque not exceeding 58 Nm.

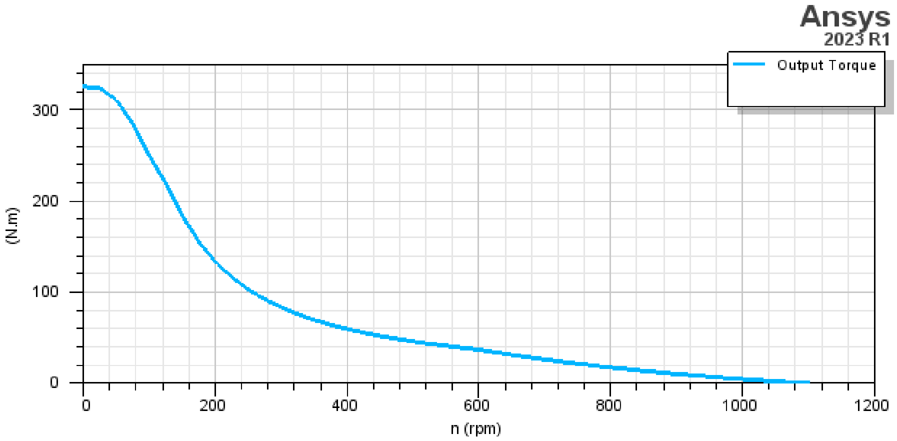

Figure 5. A4 torque chart

The superior performance of A4 is attributed to the synergistic effect of its components: the high magnetic flux density of NdFe35 generates greater electromagnetic force, while the larger wire diameter (1.6 mm) significantly reduces winding resistance, allowing higher current flow with lower losses. This enables the motor to maintain stable high torque over a wide speed range. Additionally, the use of 14 conductors ensures a balanced configuration, avoiding excessive back-EMF and winding losses that typically occur with over-wound systems.

In summary, configuration A4 is identified as the most efficient and stable setup for maximizing torque output in BLDC motors under the tested conditions.

Maximum Rotational Speed Analysis

The comparison of maximum rotational speeds among four selected BLDC motor configurations is presented in Figure 6, based on RMxprt simulation results.

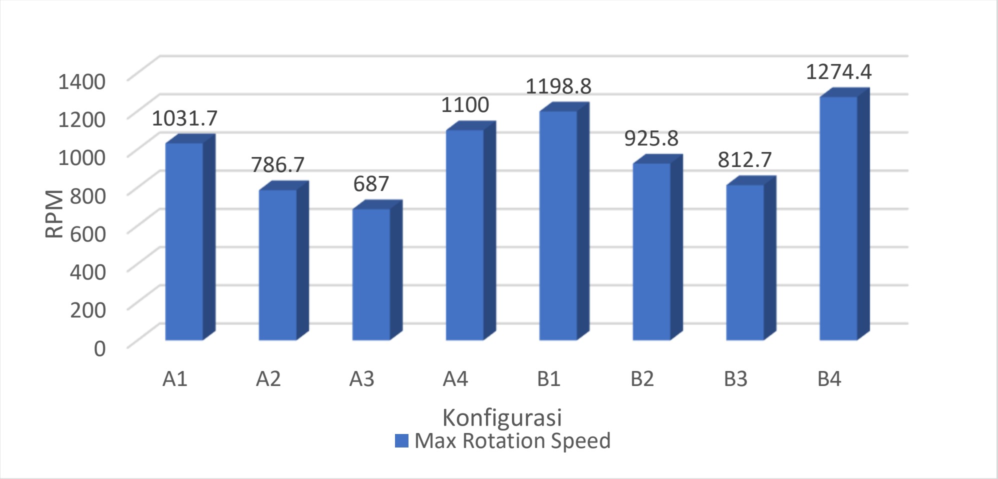

Figure 6. Rotational speed diagram

As shown in Figure 6, the highest rotational speed was achieved by configuration B4 (SmCo24 magnet, 14 conductors, 1.6 mm wire diameter) at 1274.4 rpm, followed by B1 (SmCo24, 15 conductors, 1.45 mm) at 1198.8 rpm, and A4 (NdFe35, 14 conductors, 1.6 mm) at 1100 rpm. The lowest speed was recorded in configuration A3 (NdFe35, 23 conductors, 1.3 mm), reaching only 687 rpm.

These differences in rotational speed are primarily influenced by the magnetic field characteristics of the permanent magnet materials and the winding parameters, including the number of conductors and wire diameter. SmCo24, having a weaker magnetic field than NdFe35, produces a lower back-electromotive force (back-EMF), allowing the motor to reach higher speeds before being limited by counter-voltage effects. In contrast, NdFe35, with its stronger magnetic field, generates a higher back-EMF, which tends to restrict the motor's maximum speed.

In addition, the number of conductors per slot and wire diameter play crucial roles. Configurations with fewer conductors, such as A4 and B4 (both with 14 conductors), achieved higher rotational speeds than configurations with 23 conductors, such as A3 and B3. This is because more windings increase coil resistance and induced voltage, leading to reduced motor speed due to greater electrical losses and counter EMF. In summary, configurations featuring lower winding counts and permanent magnets with reduced back-EMF characteristics are more suitable for high-speed applications, where maximizing rotational velocity is a key performance requirement.

Efficiency and Maximum Output Power

The simulation results for motor efficiency and maximum output power across the eight BLDC configurations are presented in Table 5, comparing combinations of NdFe35 and SmCo24 permanent magnets.

Table 5. Efficiency and maximum output power

Configuration	***Efficiency (%)***	***Maximum output power(kW)***
A1	78	2.7
A2	80	2.02
A3	81	1.71
A4	79	2.91
B1	75	2.26
B2	78	1.68
B3	78	1.46
B4	76	2.44

The data show that configuration A4 (NdFe35 magnet, 14 conductors, 1.6 mm wire diameter) achieved the highest performance, with an efficiency of 79% and a maximum power output of 2.91 kW. Among the other NdFe35-based configurations, A2 recorded the highest efficiency at 80%, but delivered only 2.02 kW of output power. Similarly, A3 achieved 81% efficiency, yet produced the lowest output power among the NdFe35 group, at just 1.71 kW. These findings indicate an inverse relationship between the number of windings and output power. While increased winding count may improve efficiency due to reduced core losses, the corresponding rise in winding resistance can significantly reduce the overall output power.

In contrast, configurations using SmCo24 magnets (B1–B4) generally demonstrated lower efficiency and output power compared to their NdFe35 counterparts. Configuration B1 (15 windings) reached an efficiency of 75% with a maximum power of 2.26 kW, while B2 (20 windings) dropped to 68% efficiency and 1.68 kW output. Although B3, which used a higher winding count, attained 78% efficiency, it generated the lowest power output in the group, at 1.46 kW. B4, which combined a unique winding count and wire diameter, reached 76% efficiency and 2.44 kW of output power.

Overall, the results confirm that NdFe35 offers a clear performance advantage over SmCo24, particularly in terms of output power. This can be attributed to its superior magnetic properties namely, higher remanent flux density and maximum energy product (BHmax) which enable the motor to generate a stronger and more stable magnetic field. These characteristics enhance overall motor performance, positioning configuration A4 as the most optimal design among all configurations evaluated in this study.

Maximum and Average DC Input Current Analysis

Table 6 and Figure 7 present the maximum and average DC input current consumed by the BLDC motor across different configurations, based on variations in permanent magnet type and winding parameters. The simulation results show that configuration A4 (NdFe35 magnet, 14 conductors, Ø 1.6 mm) consumed the highest current, with a peak current of 1401 A and an average current of 146.8 A. This reflects the motor's substantial power demand, which correlates with its superior torque and maximum output power. Configuration A1 (15 conductors) recorded a peak current of 1074.3 A and an average of 144.4 A, while A2 (20 conductors) showed a significant drop to 805.7 A (max) and 106.6 A (avg). The lowest current was recorded in A3 (23 conductors, Ø 1.3 mm), with 563.3 A (max) and 86.5 A (avg).

Table 6. Input DC current

Configuration	Highest DC input value	Average DC input
A1	1074.3 A	144.4 A
A2	805.7 A	106.6 A
A3	563.3 A	86.5 A
A4	1401 A	146.8 A
B1	1074.3 A	128.9 A
B2	805.7 A	94 A
B3	563.2 A	76.7 A
B4	1401 A	146.8 A

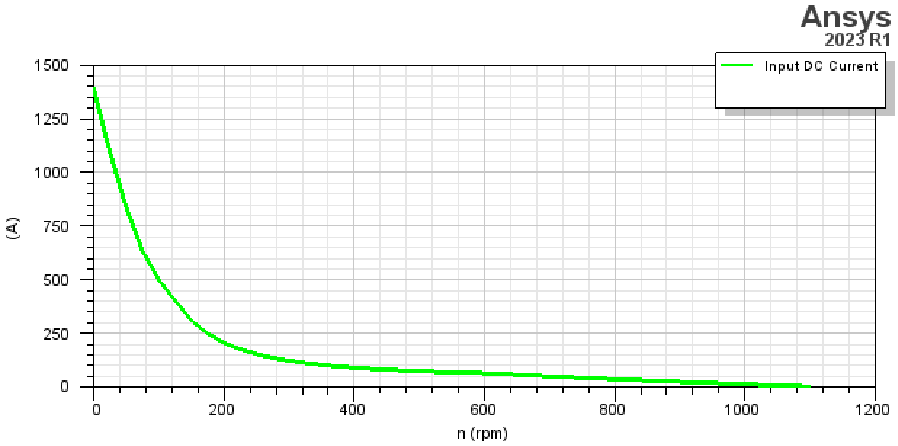

Figure 7. A4 DC current input chart

A similar trend is observed among SmCo24-based configurations. Configuration B4 also recorded a peak current of 1401 A and an average of 146.8 A, matching the performance of A4. Meanwhile, B1 (15 conductors) consumed 1074.3 A (max) and 128.9 A (avg), while B2 (20 conductors) further dropped to 805.7 A (max) and 94 A (avg). B3 showed the lowest values, with a peak current of 563.2 A and an average of only 76.7 A. This phenomenon can be explained using Ohm's Law, where an increase in winding turns leads to higher coil resistance. For a fixed input voltage, increased resistance results in lower current flow. While reduced current may seem beneficial, it can be counterproductive; higher resistance increases power loss due to heat (I^2R losses), ultimately decreasing motor efficiency. Thus, configurations with higher current draw, such as A4, may be less energy-efficient but offer superior output in terms of torque and power, making them the most balanced in terms of input–output performance.

From the perspective of magnet material, NdFe35 configurations consistently consumed more current than SmCo24 counterparts with the same number of turns. This is due to the stronger magnetic field strength produced by NdFe35, which drives the motor to operate at higher torque and power levels, thereby increasing its current demand accordingly.

CONCLUSION

Conclusion

This study investigated the electromagnetic performance of BLDC motors for lightweight electric vehicle applications through variations in permanent magnet type, wire diameter, and conductor count per slot. Among eight simulated configurations, A4 featuring NdFe35 magnets, 14 conductors, and 1.6 mm wire diameter demonstrated the best overall performance, achieving the highest torque (325 Nm), output power (2.91 kW), and competitive efficiency (79%). The results show that NdFe35 outperforms SmCo24 in generating torque and power, due to its stronger magnetic flux density. Additionally, lower conductor counts and larger wire diameters reduce winding resistance, allowing greater current flow and higher output. Although configurations with more windings slightly improved efficiency, they suffered from significant power and torque losses due to increased resistance and reduced current. In conclusion, a well-balanced design combining high-flux magnets, minimal winding resistance, and appropriate conductor sizing is key to optimizing BLDC motor performance. Configuration A4 proves to be the most effective for compact electric vehicles that require high torque, high power, and efficient operation.

REFERENCES

[1] M. Kubański, “Prospects for the Use of Electric Vehicles in Public Transport on the Example of the City of Czechowice-Dziedzice,” *Transportation Research Procedia*, vol. 44, no. 2019, pp. 110–114, 2020, doi: 10.1016/j.trpro.2020.02.016.

[2] H. El Hadraoui, M. Zegrari, A. Chebak, O. Laayati, and N. Guennouni, “A Multi-Criteria Analysis and Trends of Electric Motors for Electric Vehicles,” *World Electric Vehicle Journal*, vol. 13, no. 4, pp. 1–28, 2022, doi: 10.3390/wevj13040065.

[3] D. Mohanraj *et al.*, “A Review of BLDC Motor: State of Art, Advanced Control Techniques, and Applications,” *IEEE Access*, vol. 10, pp. 54833–54869, 2022, doi: 10.1109/ACCESS.2022.3175011.

[4] C. F. Yuliyanto and Asrori, “Pengaruh Jumlah Slot Stator Terhadap Kecepatan Putaran dan Suhu pada Motor BLDC,” *Journal of Mechanical Engineering*, vol. 1, no. 3, p. 11, 2024, doi: 10.47134/jme.v1i3.2962.

[5] E. Cetin, “Brushless Direct Current Motor Design and Analysis,” *COJ Electronics & Communications*, vol. 2, no. 2, pp. 1–13, 2021, doi: 10.31031/cojec.2020.02.000534.

[6] C. Rachael, G. Adam, and S. Andrewson, “Overview of Brushless DC (BLDC) Motors and Their Advantages Author,” no. April, 2025.

[7] R. Kurniawan, E. A. Hakim, and M. Irfan, “Analisis Pengaruh Variasi Lebar Air Gap Pada Motor Brushless DC Radial Fluks,” *Journal of Mechatronic and Electrical Enggineering*, vol. 1, no. 1, pp. 1–7, 2021, [Online]. Available: https://ejournal.umm.ac.id/index.php/JMEE/article/view/11830%0Ahttps://ejournal.umm.ac.id/index.php/JMEE/article/download/11830/9637

[8] Y. ÖZÜPAK, “Design and Analysis of Permanent Magnet DC Machines with FEM Based ANSYS-MAXWELL,” *International Journal of Innovative Engineering Applications*, vol. 7, no. 1, pp. 7–12, 2023, doi: 10.46460/ijiea.1130422.

[9] A. Sen, B. Singh, K. Mahtani, A. Moradzadeh, and S. M. Muyeen, “Results in Engineering Optimized design of a permanent magnet brushless DC motor for solar water-pumping applications,” vol. 26, no. November 2024, 2025.

[10] T. Subramani *et al.*, “Effect of Nano Urea on growth, yield and nutrient use efficiency of Okra under tropical island ecosystem,” *International Journal of Agricultural Sciences*, vol. 19, no. RAAAHSTSE, pp. 134–139, 2023, doi: 10.15740/has/ijas/19.raaahstse-2023/134-139.

[11] F. Ferdyanto, G. Fatwa, A. Erlangga, and I. Marbawi, “Performance Analysis of Permanent Magnet BLDC Motor for Reducing Cogging Torque Using Taguchi Method,” *Elkha*, vol. 16, no. 1, p. 28, 2024, doi: 10.26418/elkha.v16i1.76582.

[12] Y. L. Karnavas, I. D. Chasiotis, and A. D. Gkiokas, “An Investigation Study Considering the Effect of Magnet Type, Slot Type and Pole-Arc to Pole-Pitch Ratio Variation on PM Brushless DC Motor Design,” *Proceedings - 2018 5th International Conference on Mathematics and Computers in Sciences and Industry, MCSI 2018*, pp. 7–13, 2018, doi: 10.1109/MCSI.2018.00010.

[13] C. Zhu, R. Lu, C. Mei, T. Peng, G. Zhang, and F. Aymen, “Design and Simulation Analysis of Stator Slots for Small Power Permanent Magnet Brushless DC Motors,” *International Transactions on Electrical Energy Systems*, vol. 2023, 2023, doi: 10.1155/2023/1152243.

[14] A. Kumar, R. Gandhi, R. Wilson, and R. Roy, “The impact of different slot design of BLDC motor in a complete drive system,” *IECON Proceedings (Industrial Electronics Conference)*, vol. 2020-Octob, pp. 4300–4305, 2020, doi: 10.1109/IECON43393.2020.9255391.

[15] M. S. Raja and B. Geethalakshmi, “Modified Rotor Material for Minimization of Torque Ripple for Interior Permanent Magnet BLDC motor,” *Mater Today Proc*, vol. 5, no. 2, pp. 3639–3647, 2018, doi: 10.1016/j.matpr.2017.11.614.

[16] S. H. Susilo *et al.*, “STUDY OF STATOR SLOT CONFIGURATION AND COIL DIAMETER ON BLDC MOTOR,” vol. 1, no. 1, pp. 15–20, 2025, doi: 10.15587/2706-5448.2025.323779.

[17] J. Hao, S. Suo, Y. Yang, Y. Wang, and W. Wang, “Investigation on the relationship between winding wire size and total loss of BLDC,” *J Phys Conf Ser*, vol. 1187, no. 2, 2019, doi: 10.1088/1742-6596/1187/2/022032.

[18] A. Sauky *et al.*, “Jurnal Sauky Terbit,” vol. 10, no. 2, pp. 2–4, 2021.

[19] Ansys, “Maxwell Help,” *© ANSYS, Inc.*, no. January, p. 2955, 2019.

[20] Ing. Jan Hlúbik, “Czech Technical University in Prague Faculty of Electrical Engineering Department of Cybernetics,” no. September, p. 49, 2005, doi: 10.13140/RG.2.1.2601.1764.

[21] L. Knypiński, A. V. Reddy, B. Venkateswararao, and R. Devarapalli, “Optimal design of brushless DC motor for electromobility propulsion applications using Taguchi method,” *Journal of Electrical Engineering*, vol. 74, no. 2, pp. 116–121, 2023, doi: 10.2478/jee-2023-0015.

This page has been intentionally left blank